

The hot compaction behaviour of woven oriented polypropylene fibres and tapes. II. Morphology of cloths before and after compaction

N.D. Jordan^a, D.C. Bassett^a, R.H. Olley^a, P.J. Hine^b, I.M. Ward^{b,*}

^a*J.J. Thomson Physical Laboratory, Whiteknights, Reading RG6 6AF, UK*

^b*Department of Physics and Astronomy, IRC in Polymer Science and Technology, University of Leeds, Woodhouse Lane, Leeds LS2 9JT, UK*

Received 1 August 2002; received in revised form 22 October 2002; accepted 23 October 2002

Abstract

The morphology of woven oriented polypropylene tapes and fibres has been studied both before and after processing by hot compaction. In this technique bundles of oriented tapes or fibres are subjected to suitable conditions of temperature and pressure so that just sufficient of each tape or fibre is selectively melted; on cooling, this material recrystallizes to bind the whole structure together. Three different polymers were studied, woven into various individual weave styles, in relation to optimum processing conditions. The weave style, the adhesion between neighbouring interfaces after compaction and the direction of crack propagation along the neighbouring interfaces on peeling were examined leading to clear correlations between the observed morphology and mechanical peel strength data.

© 2002 Published by Elsevier Science Ltd.

Keywords: Polypropylene fibres and tapes; Morphology; Hot compaction

1. Introduction

Polymer/polymer composite production has been reported using numerous techniques [1–3]. This paper focuses on the morphology of single polymer composites of polypropylene (PP) formed through hot compaction, a manufacturing process developed at Leeds University, originally for polyethylene [4–6], but extended to PP [7,8]. The hot compaction process involves taking an array of oriented fibres and tapes and subjecting them to suitable conditions of temperature and pressure so that a thin skin of each individual fibre or tape is selectively melted. This molten material recrystallizes on cooling to bind the whole structure together. The resulting structure is therefore composed of a single, identical, polymeric material, with excellent fibre matrix adhesion. Although this process was initially developed for high modulus polyethylene this paper investigates the morphology of a number of polypropylene fibres, tapes and woven cloths known to be more cost effective and potentially provide a wide range of applications. Each material is of known molecular weight and polydispersity.

In a companion publication [9] we described an investigation into the compaction behaviour of a number of commercially available woven polypropylene cloths. The main thrust of this work was to establish the important variables which control the hot compaction behaviour of woven polypropylene. The paper concluded that while the mechanical properties of the melted and recrystallised phase were vitally important, other geometric parameters such as the shape of the oriented reinforcement (whether fibres or tapes) and the weave style were also important. For instance the peel load, which is the force required to peel apart two adjacent layers of the compacted composite, was found to be significantly affected by the weave style of the cloth used and the direction of peeling, i.e. either parallel to the warp or weft threads. In this paper we describe a more detailed study of these geometric aspects and how they affect the hot compaction behaviour.

2. Experimental

2.1. Materials

The materials studied are compactions made at the optimum temperature from four different cloths, A–D are as

* Corresponding author. Tel.: +44-113-3433808; fax: +44-113-3433868.

E-mail address: i.m.ward@leeds.ac.uk (I.M. Ward).

Table 1
Properties of the woven cloths

Weave code	Weave style	Polymer M_n/M_w	Count of reinforcement/10 cm	
			Weft	Warp
A	Multifilament bundles, 1080 denier	38,500/191,000	90	60
B	Multifilament bundles, 450 denier	38,500/191,000	140	140
C	Fibrillated tape: 1×0.12 mm	55,800/290,000	90	80
D	Flat tape: 2.5×0.046 mm	56,100/325,000	60	60

described in the previous study [9], and fall into two groups. A and B are both from the same grade of PP, of lower molecular weight than C and D. They are woven from multifilament bundles of different denier, and if the warp and weft are transposed are seen to have similar weave patterns (compare Figs. 2 and 3). Cloths C and D are made of similar higher molecular weight polymers but pigmented differently: C is constructed from fibrillated tape and contains an unknown pigment of pale brown colour, while D is from flat tape and contains carbon black. The parameters of the different woven cloths are given in Table 1

2.2. Compaction treatments

The preparation of the hot compacted sheets was carried out using a single pressure process as described previously in published work on woven polypropylene [7,10]. The required number of woven layers was stacked in a matched metal mould (125 mm square) with a thermocouple placed between the central two layers to allow the actual assembly temperature to be measured [9]. This assembly was then placed in a hot press set at the required compaction temperature, and a pressure of 2.8 MPa (400 psi) was immediately applied. Once the assembly reached the compaction temperature, it was left for a further 10 min, whereupon it was cooled to 100 °C at which point the sample was removed.

This paper concentrates solely on those specimens compacted at the optimum temperature for each material, given in Table 2. In particular, we have studied the morphologies of so-called ‘peel’ specimens, namely those made from two layers of cloth, with a rubber sheet placed inside the mould cavity to even out the applied pressure, and

with thin strips of aluminium foil, 10 mm wide, placed at two perpendicular sides and between the layers to act as a starting crack on subsequent peel testing, parallel to weft and warp. All the specimens discussed here were compacted with the warp and weft fibres in both layers aligned, normally termed a 0/0 layup. There are also layers of aluminium foil placed between the rubber and the cloth to aid release of the sample and to produce a good surface finish: the machine lines of this aluminium foil become imprinted on the outer surfaces of these compactations.

2.3. Specimen preparation for microscopy

Five procedures were adopted in order to prepare specimens for scanning electron microscopy (SEM).

1. Almost square rectangles (in order to preserve the distinction between warp and weft directions) were cut from the original cloths and photographed directly at lower magnification under the SEM. The weave patterns were viewed both looking vertically down onto the cloth, and at the cloth tilted with one of the corners of the rectangle facing the observer.
2. The cloths were embedded and after etching the weave patterns were studied at higher magnification in cross-section, in one or other of the weft and warp directions. The aim here was to study of variations in alignment between two or more layers of material, and its ability to interlock in both warp and weft directions. In the main method, a sheet measuring 5 mm \times 5 mm was cut from the bulk material and embedded between two sheets of Kraton[®] block copolymer: this is shown in Fig. 1(a). In another method, the material was embedded between high impact polystyrene using an epoxy resin consisting

Table 2
Mechanical properties of the compactations

Weave code	Compaction temperature (°C)	Tensile modulus (GPa) Weft/Warp		Tensile strength (MPa) Weft/Warp		Average peel load (N/10 mm)	
		Weft	Warp	Weft	Warp	Weft	Warp
A	182	3.9	2.2	125	44	1.7 ± 0.3	3.8 ± 0.5
B	180	2.7	4.1	60	86	2.0 ± 0.4	1.3 ± 0.2
C	187	2.9	2.9	135	70	6.4 ± 0.6	7.6 ± 1.8
D	181	3.0	3.0	60	60	12.2 ± 3.9	–

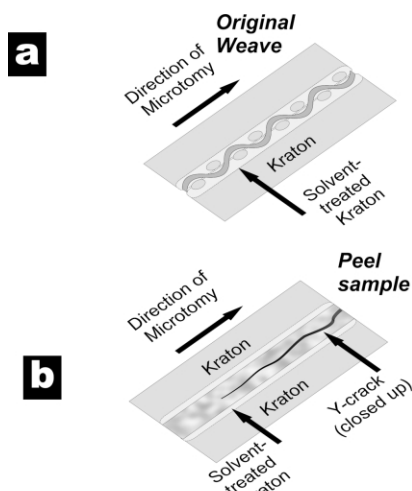


Fig. 1. Diagrams of specimen preparation.

of 17:1 Araldite MY 750 with Araldite Hardener HY 951 by weight. Each specimen was left to set overnight, and the resulting sandwich was cross-sectioned in a microtome using a glass knife cooled with dry ice in order to minimize surface damage.

Samples that had been compacted were examined in three ways:

3. Taking a compacted sample and pulling the material apart at its interfaces created peel surfaces, simultaneously allowing mechanical measurements of peel strength according to ASTM D1876, and leaving peel surfaces for examination under the SEM. Peel specimens were generated by tearing apart both parallel to the weft and warp directions. Complete details are given in the previous paper [9].
4. The outer surfaces of each peel sample were examined directly without etching, taken from a peel region adjacent to the inner peel surface specimen.
5. The peel specimens from method 3 were closed up before being embedded in a block copolymer Kraton®, the interior surfaces of which had been softened with toluene, which was allowed to evaporate overnight, after which the specimen was cross-sectioned with the glass knife microtome. The specimens were then etched, the Kraton being attacked at approximately the same rate as the polypropylene, thus preventing the side surfaces of the specimen from being eroded. This gives a side-on view of the peel surface and the route of its propagation, and is shown in Fig. 1(b).

Etching was, in general, carried out with a published permanganic reagent [8] consisting of 1% (w/v) potassium permanganate in a mixture of 10 vol concentrated sulphuric acid, 4 vol orthophosphoric acid (min 85%) and 1 vol water. Etching time was 2 h, after which the specimens were recovered by the published procedure. The only exception was the specimens embedded in Araldite, which were

etched for 15 min in the mixture recommended for isotactic polystyrene [11].

All specimens were sputter coated with gold and examined under a Phillips 515 (SEM). All were mounted at 0°, all compressed, peeled, and Y-sections were further rotated by 45° and then tilted by 45° for better contrast and to display both directions of the weave equally.

3. Results and discussion

3.1. Raw materials

The cross-sections of the original weaves indicate the importance of alignment of numerous layers during processing. In many cases the weave was said to be balanced resulting in the cross-sections viewed in both the warp and the weft direction to contain an equal amount of fibres. The weave pattern and the amount of crimp that is caused during production in one or both the weft and warp directions can have a direct effect on the force required to ‘peel’ two or more layers apart, by causing a geometric effect when the layers are laid against each other during hot compaction. In Figs. 2–5 the weft direction on each cloth is indicated by a white arrow.

Cloth A. Fig. 2 shows this viewed both parallel and perpendicular to the weft. In Fig. 2(b) the warp fibre bundles are widely spaced, and show little if any crimp, with the weft bundles alternating above and below the warp. This creates gaps between neighbouring warp bundles, encouraging good interlocking and surface adhesion between layers if they are aligned correctly (0/0 layup), but has the potential for poor registration if the alignment is poor. The extraordinary straightness of the warp fibres seen in longitudinal section bottom right of Fig. 2(c) is also confirmed in Araldite sections (not shown) in the preparation of which the fibres are held rigidly, so removing doubts over distortion otherwise occurring during sample preparation.

Cloth B. Fig. 3(a) and (b) display pictures of Cloth B, again in both directions. Cloths A and B are produced using the same polymer, but the fibre tows of Cloth B are of a lower denier, resulting in a tighter weave. This weave can be seen to display crimp in both the weft and the warp directions, though here the weft fibres are somewhat straighter, so that the general appearance of warp versus weft is reversed in relation to Cloth A. The weft bundles are also more tightly packed than the warp bundles of cloth A, and in general the bundles should fit together more neatly. This creates a flatter pattern in comparison with Cloth A, in both directions, so alignment of layers of this weave should not be so critical.

Cloth C. (Fig. 4) is woven from fibrillated tape bundles, and although at first glance it appears symmetrical, closer examination, particularly of Fig. 4(b), shows that the degree of crimp in the warp is considerably higher than the weft.

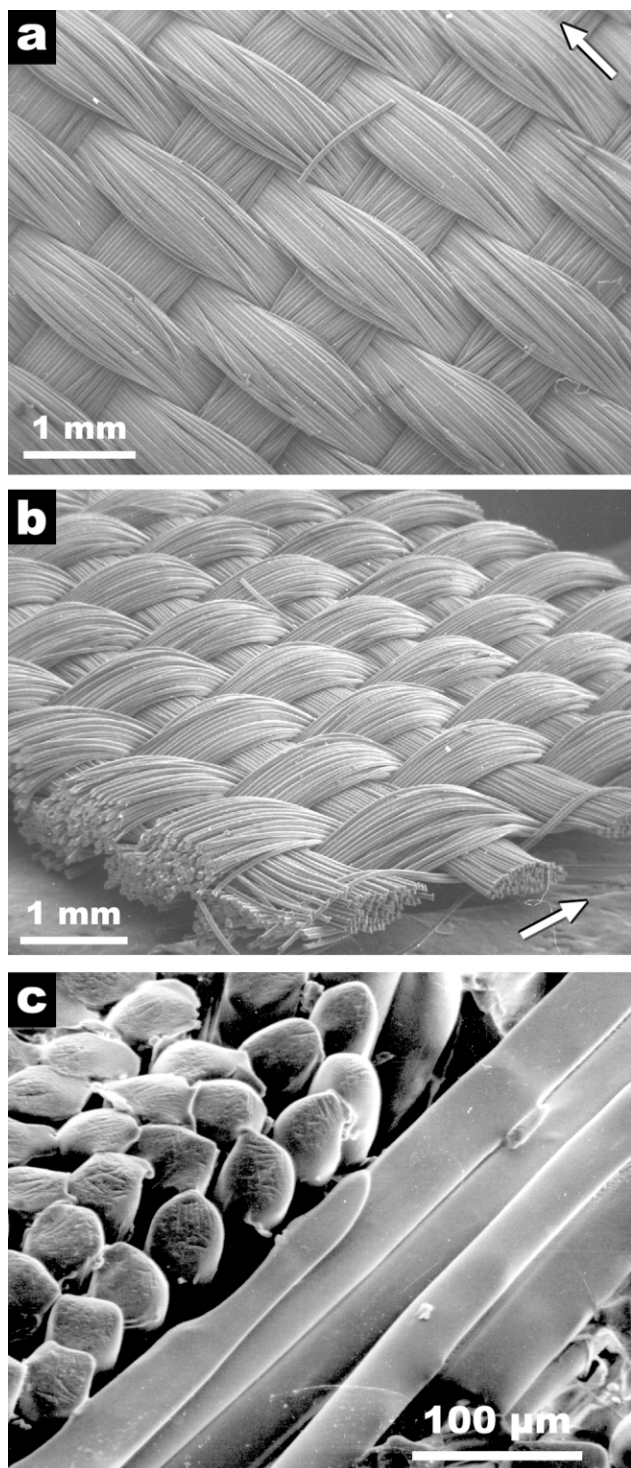


Fig. 2. Views of Cloth A. Original at low magnification (a) flat-on (b) tilted 74° (c) etched cross-section at higher magnification, tilted 45°. Arrow indicates weft direction.

Fig. 4(c) shows a few warp fibres at top left in longitudinal section. Most of the figure is taken up with weft fibres in transverse section. These are showing a tendency to fibrillate further, with many cracks which are being opened up further by the etchant.

Cloth D. Fig. 5 is made of wide flat tapes. It has a very

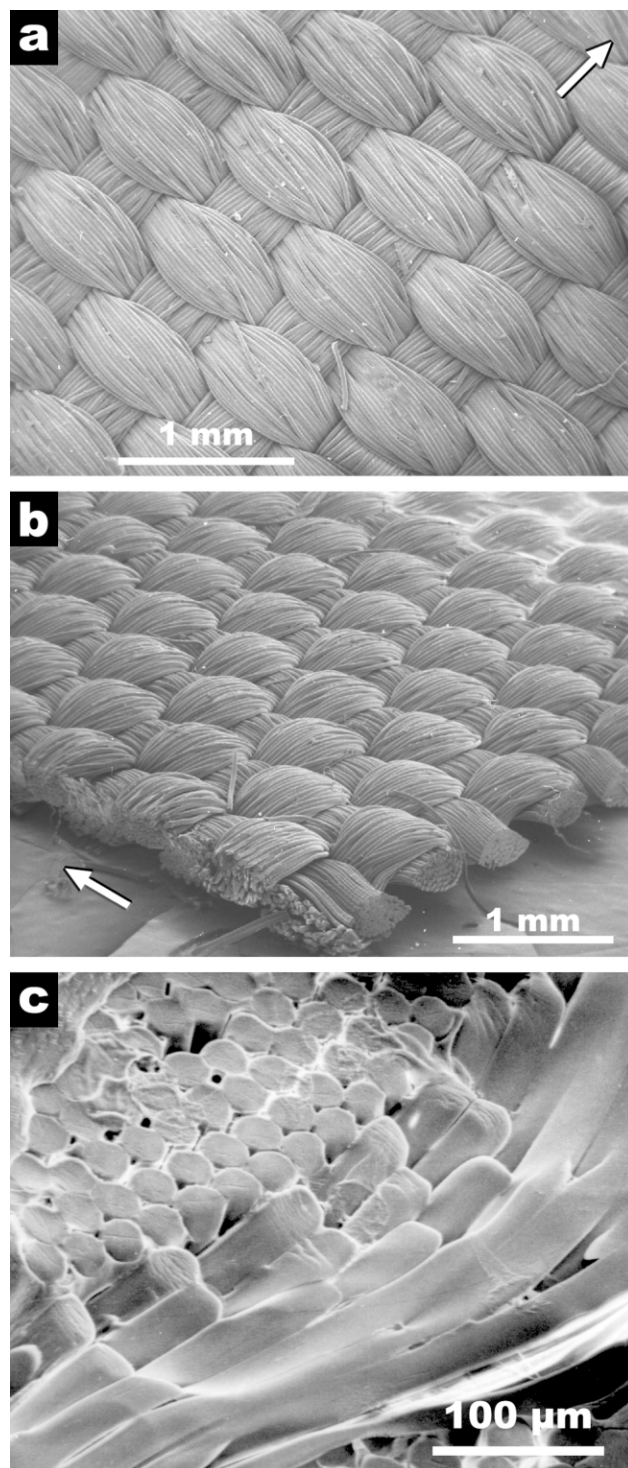


Fig. 3. Views of Cloth B. Original at low magnification (a) flat-on (b) tilted 74° (c) etched cross-section at higher magnification, tilted 45°. Arrow indicates weft direction.

loose texture, and tended to open up when sectioned in Kraton, so instead a cut surface of a specimen embedded in Araldite is shown in Fig. 5(c). The longitudinal fibres at the top show a periodic banding, sometimes seen in PP fibres [12,13] and elsewhere referred to as 'Pisa' structure from its visual appearance in etched highly drawn polyethylene

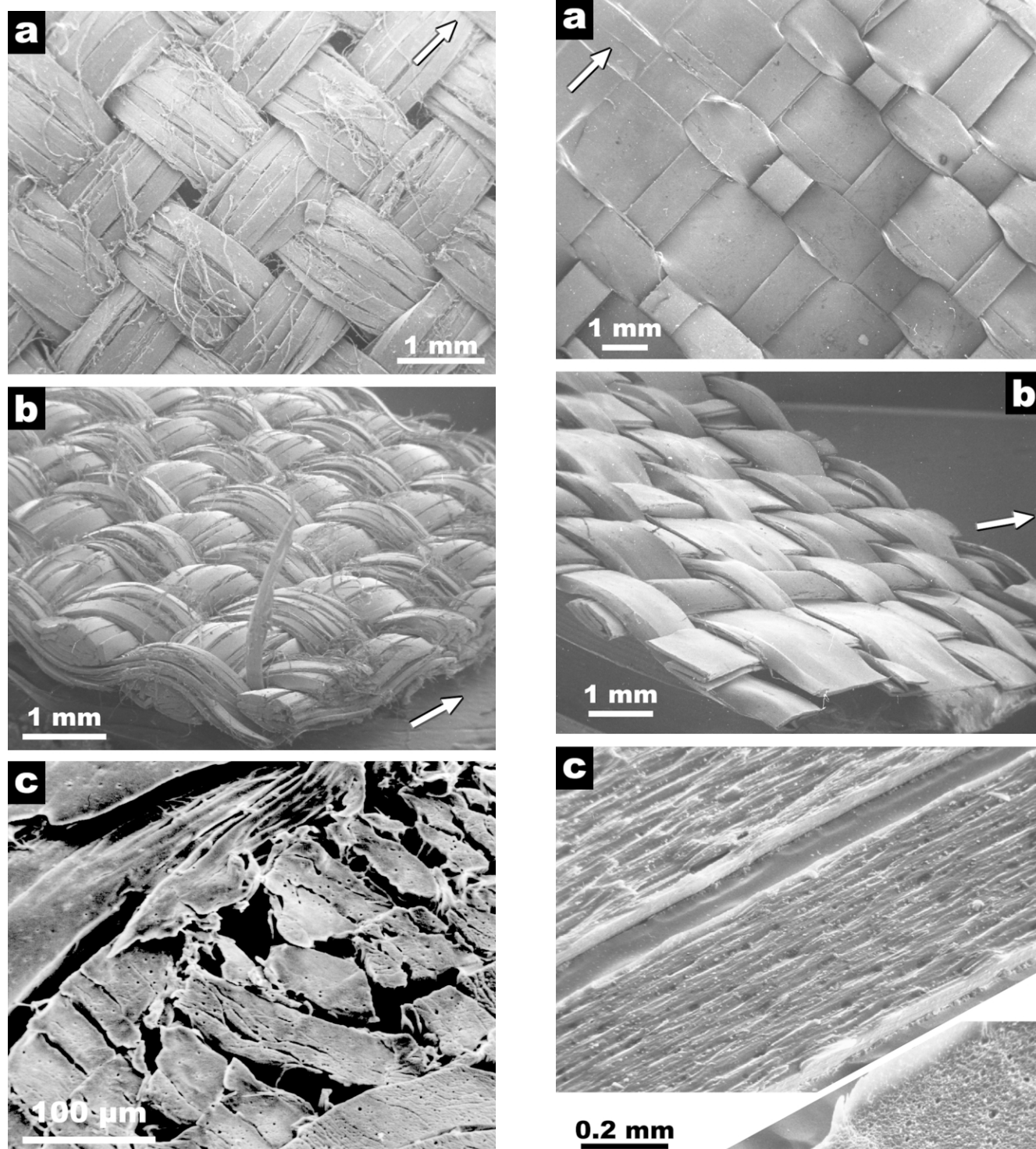
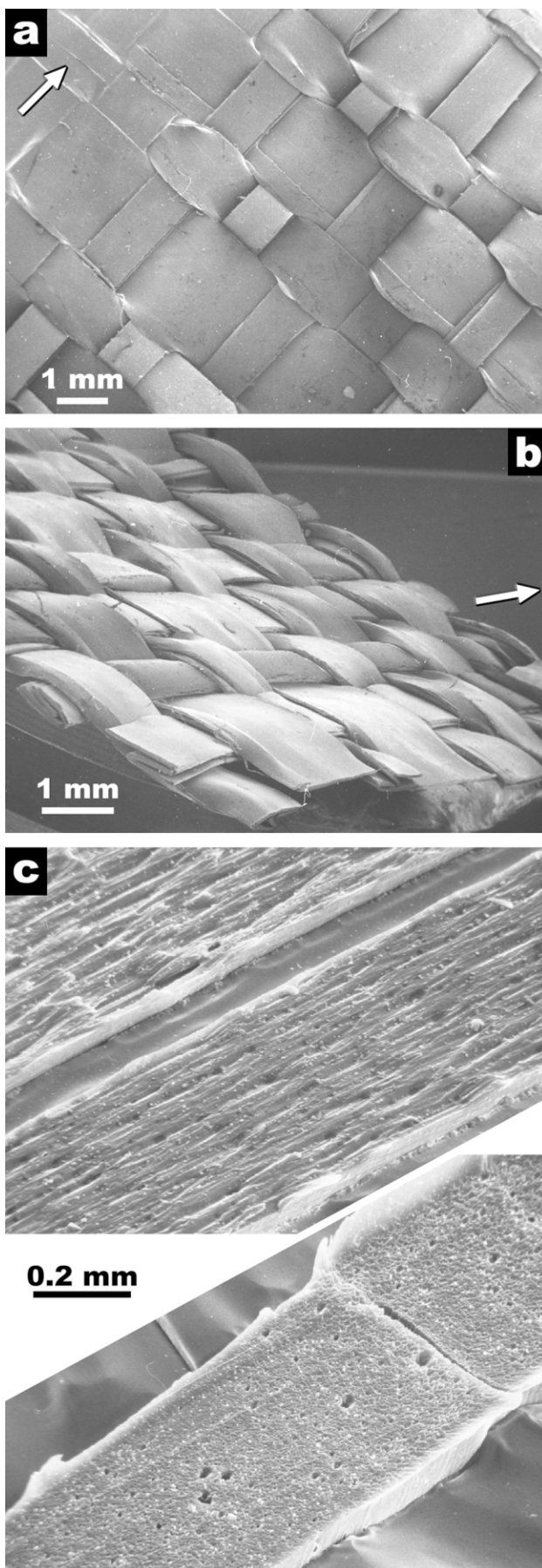


Fig. 4. Views of Cloth C. Original at low magnification (a) flat-on (b) tilted 74° (c) etched cross-section at higher magnification, tilted 45°. Arrow indicates weft direction.

Fig. 5. Views of Cloth D. Original at low magnification (a) flat-on (b) tilted 74° (c) etched cross-section at higher magnification, tilted 45°. Arrow indicates weft direction.



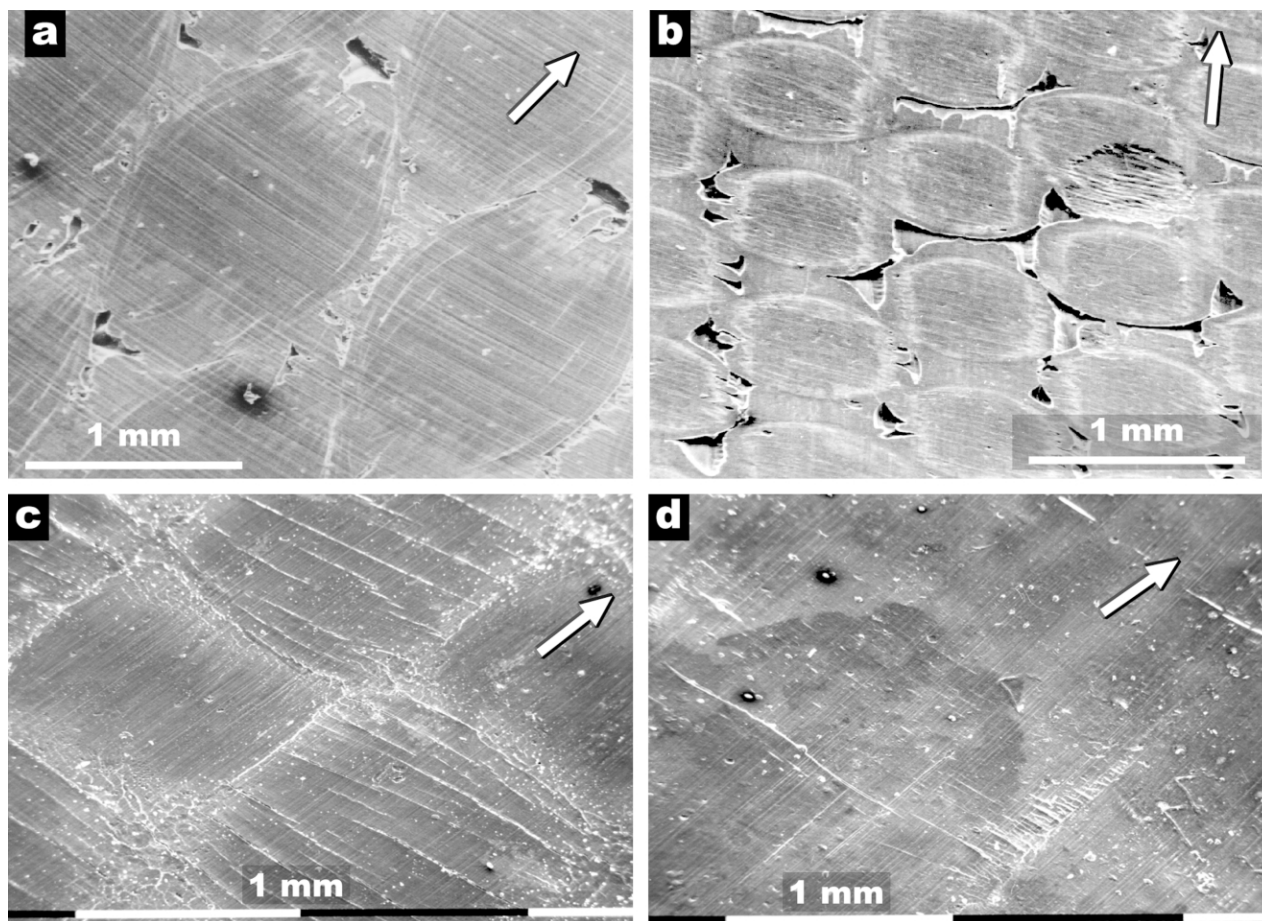


Fig. 6. Low magnification views of pressed surfaces opposite peel surfaces (a) Cloth A (b) Cloth B (c) Cloth C (d) Cloth D. Arrows indicate weft direction.

specimens [14]. Because Araldite is much more rapidly attacked by the reagent, the etching time has to be rather short, and so the characteristic morphology of the 'Pisa' structure is perhaps not fully developed.

3.2. Outer surfaces of compacted sheets after peel testing

The compacted outer surfaces of all materials studied are shown in Fig. 6: on these pictures, the white arrow indicates the direction of peeling. These are segments taken from specimens peeled parallel to the weft. All surfaces show parallel striations which are a cast of the aluminium foil sheets against which they were compacted: the direction of these lines has no significance. Those made from Cloths A and B (Fig. 6(a) and (b)) display a strongly superimposed image of the underlying weave pattern. Besides the weave pattern there are large holes which have developed as a result of the melt retreating whilst the material has cooled from the compaction temperature. This is an indication of the presence of a low MW tail in the MW distribution of the polymer, giving a low melting fraction which floods the specimen at the compaction temperature. The compressed surface of Cloth C (Fig. 6(c)) is somewhat different in that it contains numerous cracks running through the surface perpendicular to the peel direction, which occur in

alternating squares in a checkerboard pattern. They happen to be where the warp forms the outer surface, but although the warp is slightly more crimped than the weft this is not the chief explanation. It is, rather, that as the peel specimen is pulled apart, the strip develops cylindrical curvature around the warp direction, and the tensile stresses so developed has given rise to fibrillation and transverse cracking. In some parts of the same specimen the peel strip has buckled across its width rather than length, and here it is the weft bundles which tend to crack, though not as much as the warp ones. An appearance of bright 'dusting' at the boundaries of the squares is due to lower molecular weight exudates, but this is much less in quantity than in Cloths A and B. Cloth D shows a little cracking, but otherwise only a rectangular pattern from the fibre bundles. Cloth C appears much more prone to fibrillation, and this is perhaps a reflection of the original process used to make the tape, which requires this material to fibrillate.

3.3. Peel surfaces

The peel surfaces are shown next. Again their properties give a natural division of the materials into two sets of two, which are shown in Fig. 7 for the Cloths A and B, and Fig. 8 for Cloths C and D.

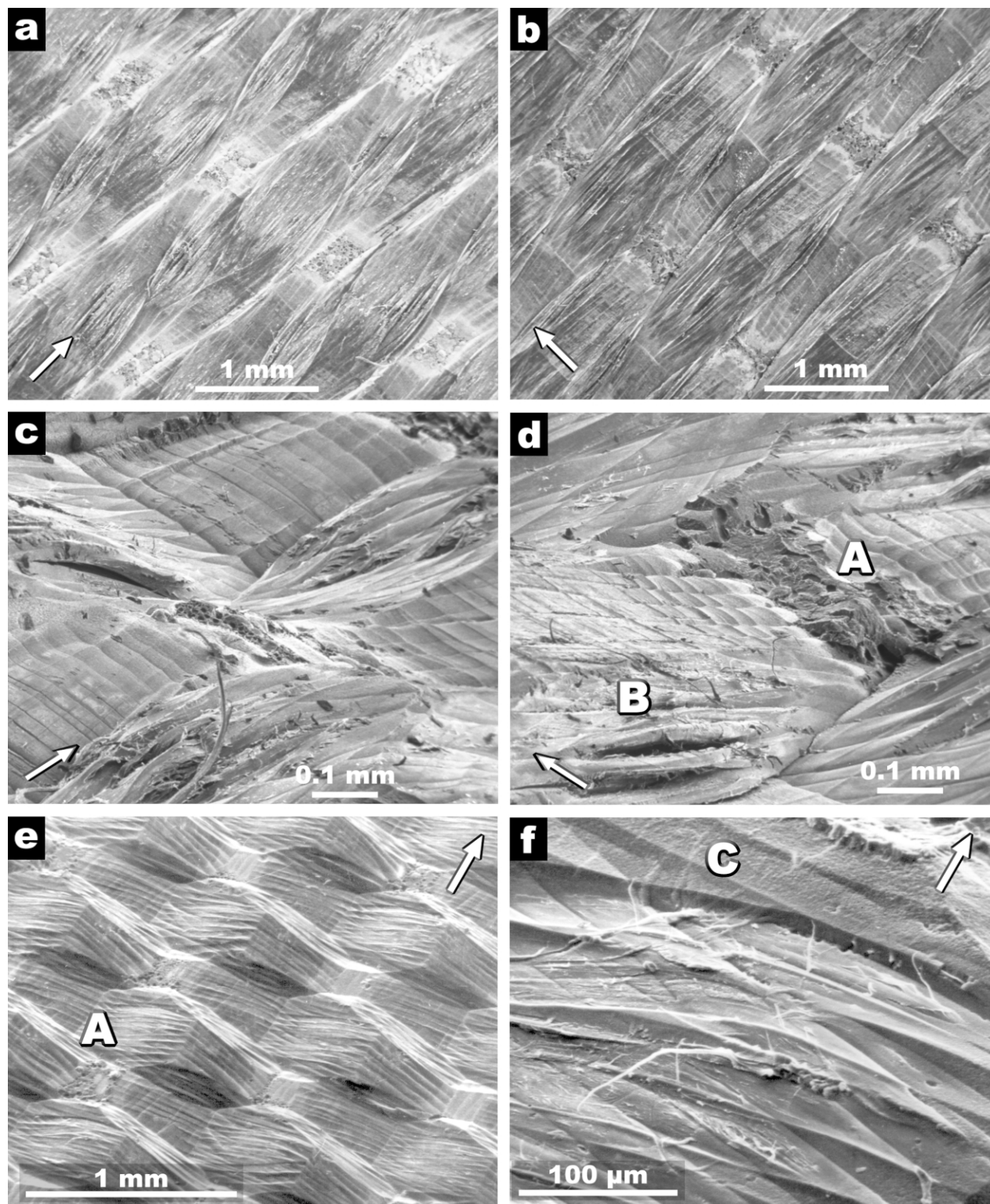


Fig. 7. Views of peel surfaces: direct views of Cloth A with peel direction arrowed (a) parallel to weft and (b) parallel to warp. Higher magnification views tilted at 74° (c) peeled parallel to weft (d) parallel to warp. Cloth B tilted 45° (e) low magnification and (f) higher magnification.

Fig. 7(a) and (b) give a direct view of cloth A, peeled parallel to the weft (a) and parallel to the warp (b) (for Figs. 7 and 8 the white arrow indicated the peeling direction). For both of these pictures the conditions for taking the

micrographs were maintained rigidly constant, in particular magnification, gain, black level, and settings for subsequently scanning the negatives. The different orientations of the peel directions, which are mirror-imaged around the

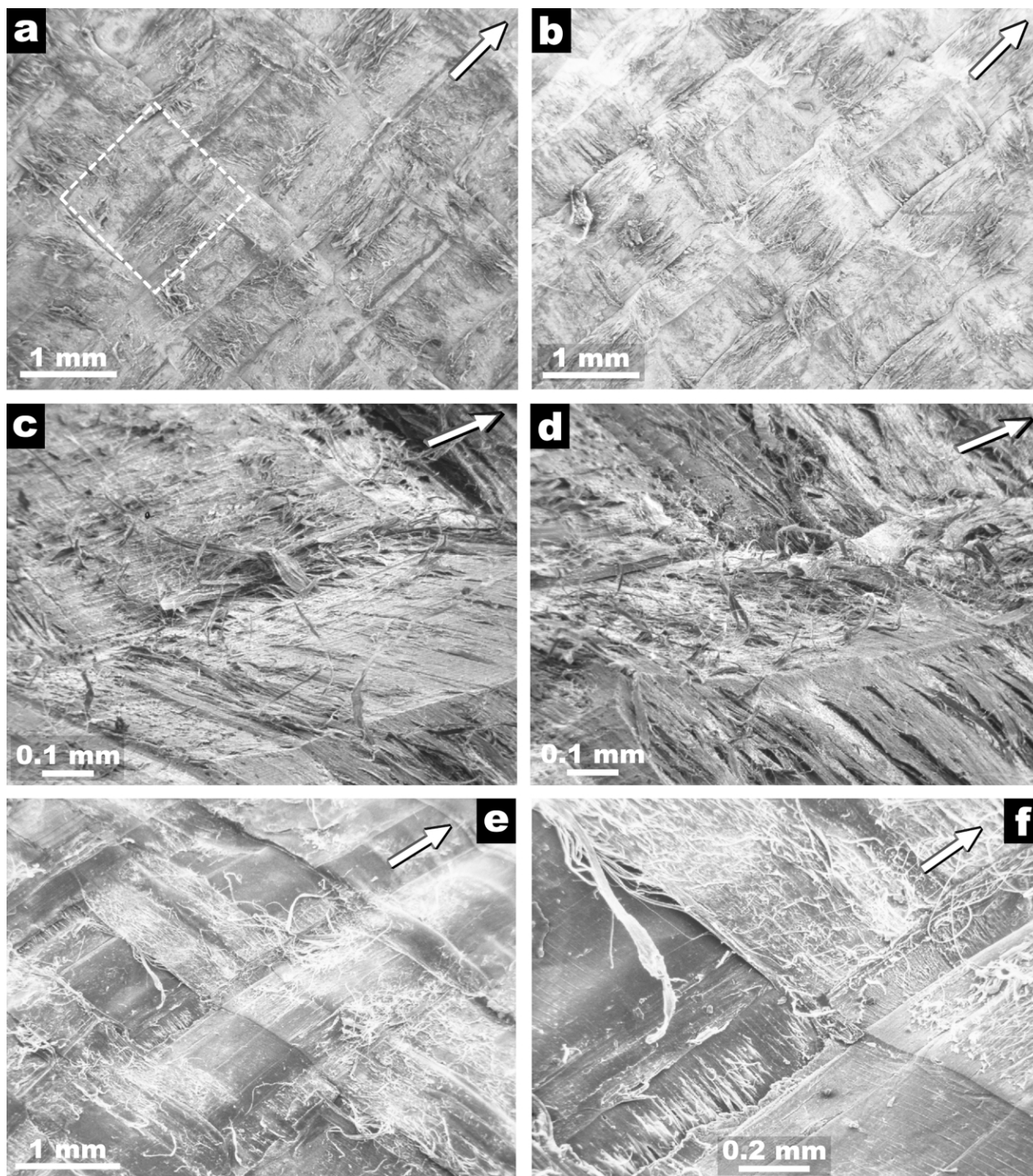


Fig. 8. Views of peel surfaces: direct views of Cloth C with peel direction arrowed (a) parallel to weft and (b) parallel to warp. Higher magnification views tilted at 74° (c) peeled parallel to weft (d) parallel to warp. Cloth D tilted 45° (e) low magnification and (f) higher magnification.

vertical, are chosen so that the warp and weft fibres in each specimen can be compared directly. There is a greater whitening observed in the specimen peeled parallel to the weft (part (a)): a similar difference in optical appearance was noted in the previous paper, but since we are here imaging with electrons there is the opportunity to study this in greater detail. Such a phenomenon would indicate greater disturbance of the surface, but such greater mechanical

damage is hard to correlate with the lower peel strength in this direction. In tilted view (parts (c) and (d)) the situation becomes clearer. Two general features are present in both peel surfaces. Firstly, it is apparent that the fibre bundles have been indented by those against which they have been pressed, and so there is a confusing appearance of fibres running in both directions over the same area. This feature is present in the compaction, but is revealed by peeling. The

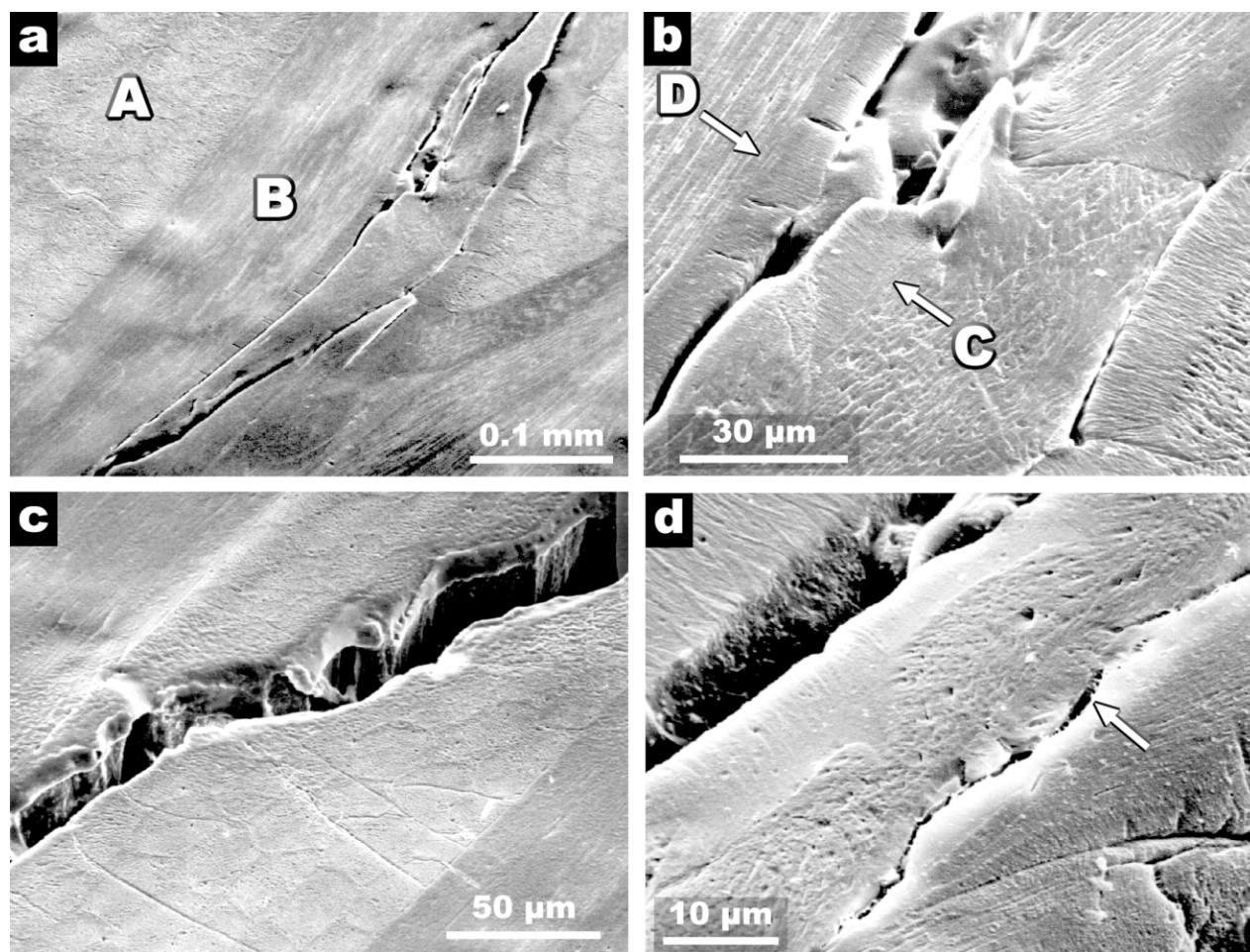


Fig. 9. Etched peel surface Y-cracks in the fibre-bundle materials. (a) and (b) Cloth A, (c) and (d) Cloth B.

other feature is areas such as that immediately below and to the left of A in Fig. 7(d), which is a small area where low molecular weight material has congregated during compaction and has recrystallised as spherulites on cooling. Such areas are also seen in parts (a)–(c) of the figures, and would correspond to the holes seen to form within the compressed surfaces of these materials as this LMW melt retracts on solidification. This material is mechanically very weak, and has suffered much damage during the peeling test: Fig. 7(d) shows how in this specimen, peeled parallel to the warp, the fibres tend to be wrenched apart (labelled B) to a greater degree than in the corresponding weft specimen of part (c): if one looks closely in Fig. 7(b) there is also greater damage visible in the transverse bundles, which look more disturbed. This would correlate well with the greater peel strength in this direction of peeling: in the first paper, this was attributed to these bundles being pulled apart by the tensile forces present when the bundles are transverse to the peeling direction, a process which absorbs more energy. Compactions of cloth B behave similarly on peeling (Fig. 7(e) and (f)). There are again areas labelled A in Fig. 7(e) of residual LMW material which has congregated in the gaps where there is the greatest mismatch between the two layers

of weave. At higher magnification the individual fibres appear to be covered as at C in Fig. 7(f) with a dusting of fine textured material, again probably low molecular weight exudate.

The peel surfaces of the Cloths C and D are displayed in Fig. 8. The dotted white square in Fig. 8(a) shows the ‘unit square’ of the cloth 3 weave, which is here divided into four rectangles arising from the offset of the weaves in the two cloths: the four segments represent weft-on-weft, warp-on-warp, weft-on-warp and warp-on-weft. The two fibre directions are not completely related to the warp-and-weft pattern of the underlying cloth because in some cases, the part of the underlying weave has been pulled away, while in others it is covered by the overlying weave. Viewed directly, the specimen peeled parallel to the warp (Fig. 8(b)) shows much more whitening than that parallel to the weft (Fig. 8(a)). These pictures are taken with exactly the same continuity of conditions as Fig. 7(a) and (b). Here there is very little difference in peel strength between the two directions; however in tilted view the weft specimen (Fig. 8(c)) tends to show fine fibrillation where the warp specimen (Fig. 8(d)) shows more detachment of larger shreds of fibre. At least in terms of mechanical strength,

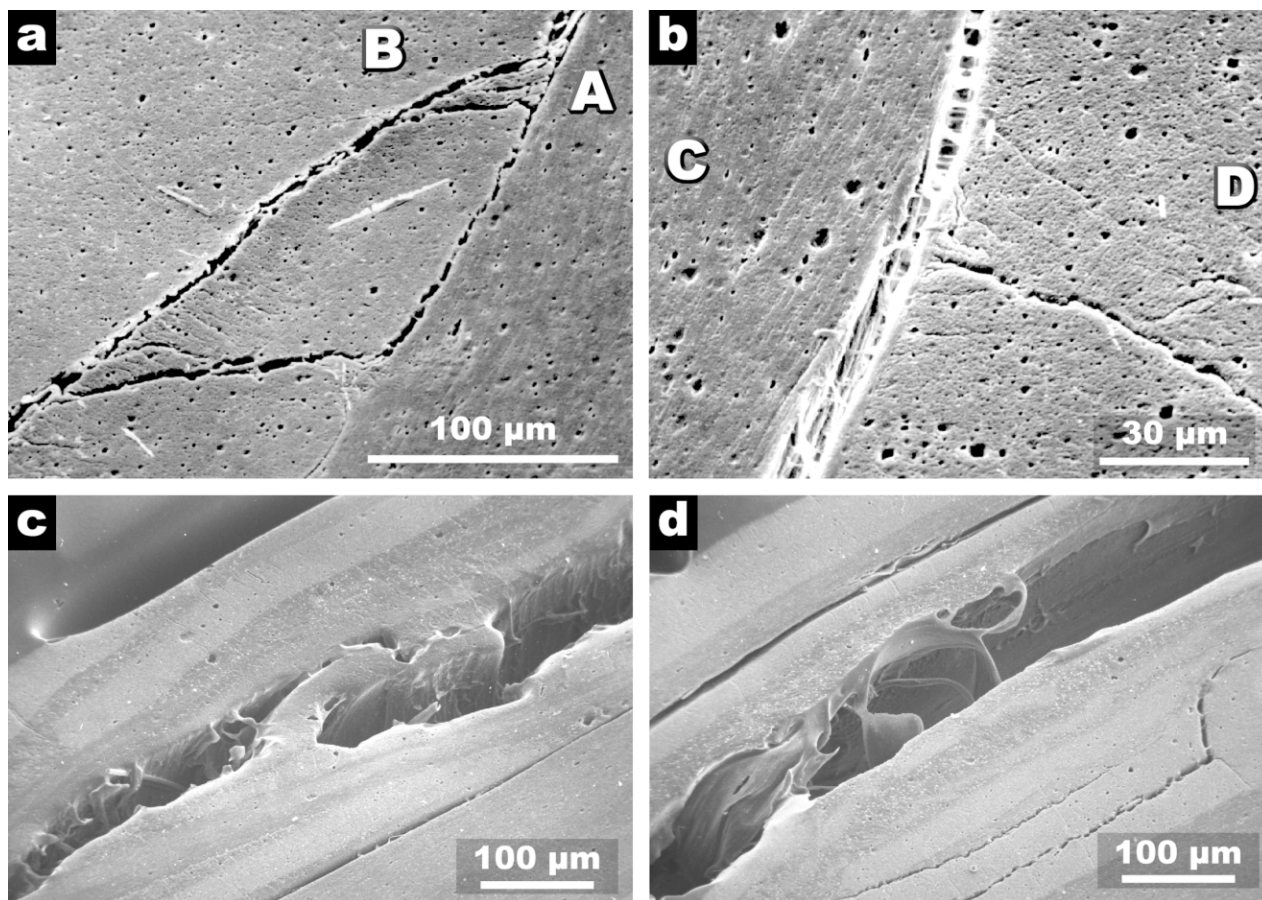


Fig. 10. Etched peel surface Y-cracks in the fibre-bundle materials. (a) and (b) Cloth C, (c) and (d) Cloth D.

these two types of fracture appear to be equal in their effect. The peel surfaces of cloth 4 are shown at two different magnifications in Fig. 8(e) and (f). In part (f) it is apparent that one of the tapes is becoming separated from the one underneath: this phenomenon will be shown more clearly later in the examination of the cross-sections of the peel surfaces. Generally cracking and fibrillation appear more extensive perpendicular to the peel direction. This may well arise from the peeled tape being rolled up this way, as was noted in Fig. 6(c) for the outer surface of cloth 3.

In comparing the peel surfaces of the two classes of cloth, a tape as in Fig. 8(c) and (d) shows much more micro level surface damage compared to Fig. 7(c), (d) or (f). This may be because fibrillation is easier in tapes; alternatively it could be a reflection of better bonding. Further information can be obtained by examining cross-sections of peeled specimens, which sheds more light on the origin of the superior mechanical properties of the tape compactions C and D.

3.4. Peel propagation

Cloth A and B are both similar in that the resulting peel paths are highly irregular and often branch. Fig. 9(a) shows Cloth A, with transverse (A) and longitudinal (B) fibre

bundles displayed: in A the circular sections of the individual fibres in A can just be discerned. Higher magnification in Fig. 9(b) with part of the longitudinal fibre bundle B at top left reveals that it is bounded by a transcrystalline layer D: the bundle on the other side of the crack is similarly bounded by a layer C, and the crack has propagated between the two transcrystalline layers. It is at the junction of these transcrystalline layers that we would expect the greatest segregation of defective or low molecular weight material: these junctions are like the impingement boundaries between spherulites, and differential melting experiments have shown that, even in the most carefully synthesized high-crystallinity polypropylenes, this phenomenon occurs to a small extent [15]. The crack in Cloth B (Fig. 9(c)) appears to be rather featureless, but at higher magnification (Fig. 9(d)) propagation through a pair of transcrystalline layers can be seen (upper left), and just to the lower right of centre an incipient crack occurs between two fibres which are mismatched in orientation and have undergone considerable distortion during the compaction. Here again there is an accumulation of featureless low molecular weight material (arrowed).

The compacted Cloths C and D, made from the higher molecular weight tapes (Fig. 10), do not show any of the paired transcrystalline layers seen in compactions of A and

B. Without these exuded low molecular weight layers, the tapes are in effect directly welded together, and this is believed to be the reason for their greater peel strength. The crack in cloth C (Fig. 10(a)) travels down from the upper right corner between longitudinally (A) and transversely (B) oriented fibres from the two cloths. It is difficult in this specimen to discern the individual bundles of the fibrillated tape. However, the main crack is seen to branch to the left, thereby not simply following the junction of the two cloths. The crack also continues to propagate for a short distance through the junction of the two cloths, but quickly diverts into B and re-joins the main crack. It is likely that the triangular region bounded by this feature would, in the actual peel surface similar to that shown in Fig. 8(d), form one of the pulled-up laths of material covering this surface. In Fig. 10(b) the opening up of the crack is seen to be accompanied by extensive fibrillation, such as that observed in other areas of Fig. 8(c) and (d), i.e. those with a more 'shredded' appearance. Where the two halves of the specimen are pushed together further back this fibrillated material forms a kind of 'stuffing' between the two surfaces. In cloth D there is much shredding of the material. How this arises is shown in Fig. 10(c), where there is a bridging piece coming adrift between the two sides. There is similar feature about 5 mm further back along the crack (not shown), but as this has opened wider one end has, of course, detached. Seen halfway between these two bridging pieces in Fig. 10(d) are shreds of plucked material, and limited cracking along other boundaries parallel to the main crack.

The factors leading to the great difference in mechanical properties between the two main classes of hot compacted materials are now more apparent. The cracks in polymers A and B travelling between transcrystalline layers indicate the poor adhesion at these points. The apparent dusting of low molecular weight exudate seen at C in Fig. 7(f), on closer inspection, may now be assigned to a transcrystalline junction. The angular structure would suggest that the fibres started to soften and deform before the compaction temperature had been reached. At the highest temperature, low molecular weight material started to exude, and on cooling this would crystallize from the angular fibre surfaces and the locus of impingement would also be an angular surface. This might also preclude any surface fibrillation. In contrast, direct adhesion between tapes would be achieved in cloth C and D, and the energy required to induce fibrillation as they are torn apart would correlate with the greater strength observed. The specimen geometry, namely the fact that C and D are made of tapes rather than round fibres also helps: in Tensylon® polyethylene the tape geometry was found to contribute significantly to the high strengths achievable with this material [6]. However, because the fibres in A and B are so easily deformed, the effect of the less favourable geometry is not as severe as it might be, but is still significant, as evidenced by the different peel strengths in two directions for Cloth A.

4. Conclusions

Morphological examination of fibre compactions made from polypropylene cloths has shown details of how the mechanical properties, which were described in the companion paper, derive both from the molecular weight of the PP, the fabric construction (fibre or tape), and the crystalline morphology produced by the hot compaction procedure, especially in regard to transcrystalline layers formed between fibres.

Lower molecular weight PP grades tend to exude much more material than higher MW PP. This material recrystallizes to give regions of lower mechanical strength than the remaining fibre. This is especially the case where the material recrystallizes as opposing transcrystalline layers, the junction of which offers a path of low resistance to peeling.

The higher molecular weight materials tend to weld tape to tape, with very little material exuded. Peel cracks therefore tend to disrupt the fibre itself, giving extensive fibrillation. This is correlated with the superior mechanical properties of these materials.

Fibre geometry is important, in that tapes naturally present a greater surface for compaction than round fibres, which have to be distorted by compression before contact is made. However, the effect in determining the final mechanical properties is less than that of molecular weight distribution.

References

- [1] Marais C, Fellard P. *Compos Sci Technol* 1992;45:247.
- [2] Pegoretti A, Ashkar M, Migliaresi C, Marom G. *Compos Sci Technol* 2000;60:1181.
- [3] Loos J, Schimanski T, Hofman J, Peijs T, Lemstra PJ. *Polymer* 2001; 42:3827.
- [4] Hine PJ, Ward IM, Olley RH, Bassett DC. *J Mater Sci* 1993;28:316.
- [5] Olley RH, Bassett DC, Hine PJ, Ward IM. *J Mater Sci* 1993;28:1107.
- [6] Hine PJ, Ward IM, Jordan ND, Olley RH, Bassett DC. *J Macromol Sci Phys* 2001;40:959.
- [7] Hine PJ, Ward IM, Teckoe J. *J Mater Sci* 1998;33:2725.
- [8] Amornsakchai T, Bassett DC, Olley RH, Hine PJ, Ward IM. *J Appl Polym Sci* 2000;78:787.
- [9] Hine PJ, Ward IM, Jordan ND, Olley RH, Bassett DC. *Polymer*, reference to 7408 JPOL.
- [10] Hine PJ, Bonner MJ, Brew B, Ward IM. *Plast Rubber Compos Proc Appl* 1998;27:167.
- [11] Bassett DC, Vaughan AS. *Polymer* 1985;26:717.
- [12] Garton A, Carlsson DJ, Sturgeon PZ, Wiles DM. *J Polym Sci Phys* 1977;15:2013.
- [13] Abo El Maat MI, Bassett DC, Olley RH, Dobb MG, Tomka JG, Wang I-C. *Polymer* 1996;37:213.
- [14] Amornsakchai T, Olley RH, Bassett DC, Al-Hussein MOM, Unwin AP, Ward IM. *Polymer* 2000;41:8291.
- [15] Weng J, Olley RH, Bassett DC, Jääskeläinen P. Submitted for publication.